US012386172B2

(12) **United States Patent**
Aoshima

(10) **Patent No.: US 12,386,172 B2**
(45) **Date of Patent: Aug. 12, 2025**

(54) **MICROMIRROR DEVICE AND OPTICAL SCANNING DEVICE**

(71) Applicant: **FUJIFILM Corporation**, Tokyo (JP)

(72) Inventor: **Keisuke Aoshima**, Kanagawa (JP)

(73) Assignee: **FUJIFILM Corporation**, Tokyo (JP)

(*) Notice: Subject to any disclaimer, the term of this patent is extended or adjusted under 35 U.S.C. 154(b) by 505 days.

(21) Appl. No.: **17/901,969**

(22) Filed: **Sep. 2, 2022**

(65) **Prior Publication Data**

US 2023/0073166 A1 Mar. 9, 2023

(30) **Foreign Application Priority Data**

Sep. 8, 2021 (JP) 2021-146275

(51) **Int. Cl.**
G02B 26/08 (2006.01)
G02B 26/10 (2006.01)

(52) **U.S. Cl.**
CPC ***G02B 26/0858*** (2013.01); ***G02B 26/101*** (2013.01)

(58) **Field of Classification Search**
CPC G02B 26/0858; G02B 26/101
(Continued)

(56) **References Cited**

U.S. PATENT DOCUMENTS

12,019,235 B2	6/2024	Naono		
2008/0285103 A1*	11/2008	Mizumoto	.... G02B 26/0858	359/199.1

(Continued)

FOREIGN PATENT DOCUMENTS

EP	3872556 A1 *	9/2021	.... G02B 26/0858
EP	4 249 985 A1	9/2023	

(Continued)

OTHER PUBLICATIONS

Extended European Search Report for European Application No. 22192004.4, dated Feb. 7, 2023.

(Continued)

Primary Examiner — Stephone B Allen
Assistant Examiner — Boutsikaris Leonidas
(74) *Attorney, Agent, or Firm* — Birch, Stewart, Kolasch & Birch, LLP

(57) **ABSTRACT**

The micromirror device includes: a mirror portion; a first support portion that swingably supports the mirror portion around a first axis; a pair of movable frames that face each other across the first axis; a second support portion that swingably supports a movable portion around a second axis; a driving portion that surrounds the movable portion and has a gap with the second support portion on the second axis; a coupling portion that couples the second support portion and the driving portion; and a fixed frame, in which, in a state where the mirror portion rotates around the first axis and an absolute value of a rotation angle is larger than 0 degrees, assuming that, in a plane orthogonal to the first axis and including the second axis, a distance between an intersection between the second axis and a straight line located on a surface of the second support portion and including each end point of the second support portion and an end part of the second support portion on a mirror portion side in a stationary state is denoted by A, and a total length of the second support portion in a direction of the second axis is denoted by L, a relationship of ⅔<A/L is satisfied.

6 Claims, 19 Drawing Sheets

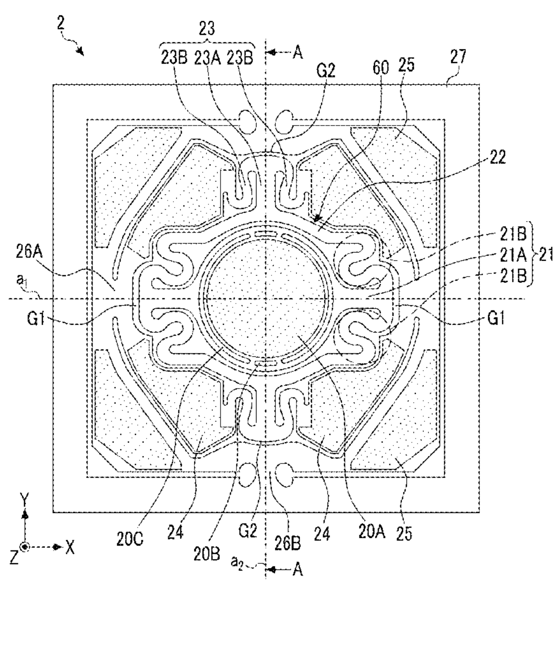

(58) **Field of Classification Search**
USPC 359/224.1
See application file for complete search history.

(56) **References Cited**

U.S. PATENT DOCUMENTS

2010/0253991	A1*	10/2010	Yamada	G02B 17/023 359/208.2
2011/0141538	A1	6/2011	Mizumoto	
2011/0181933	A1	7/2011	Kubo et al.	
2017/0210278	A1	7/2017	Matsuno	
2017/0343795	A1	11/2017	Grutzeck et al.	
2019/0265462	A1*	8/2019	Yamada	G02B 26/10

FOREIGN PATENT DOCUMENTS

JP	2017-132281	A	8/2017
WO	WO 2009/041342	A1	4/2009
WO	WO 2010/021216	A1	2/2010
WO	WO 2010/035759	A1	4/2010
WO	WO 2020/085063	A1	4/2020

OTHER PUBLICATIONS

European Communication pursuant to Article 94(3) EPC for European Application No. 22192004.4, dated Jan. 30, 2025.
Japanese Office Action for corresponding Japanese Application No. 2021-146275, dated Feb. 18, 2025, with English translation.

* cited by examiner

FIG. 1

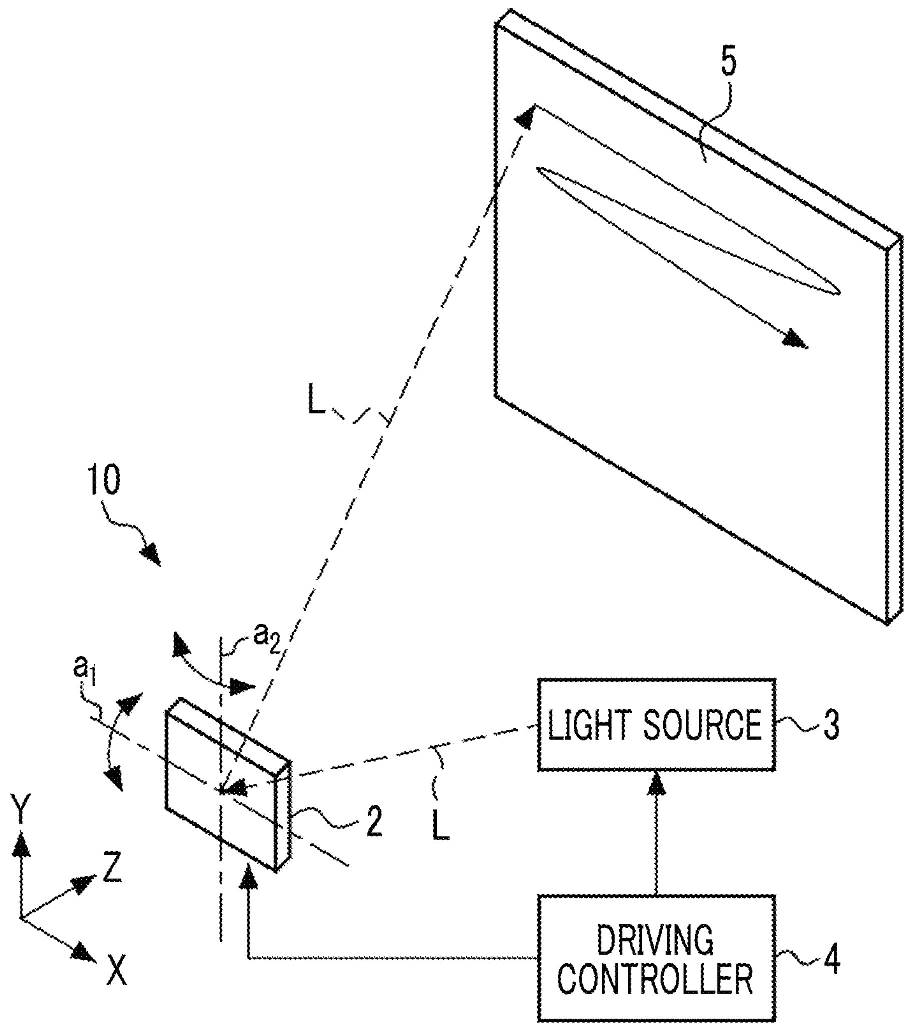

FIG. 2

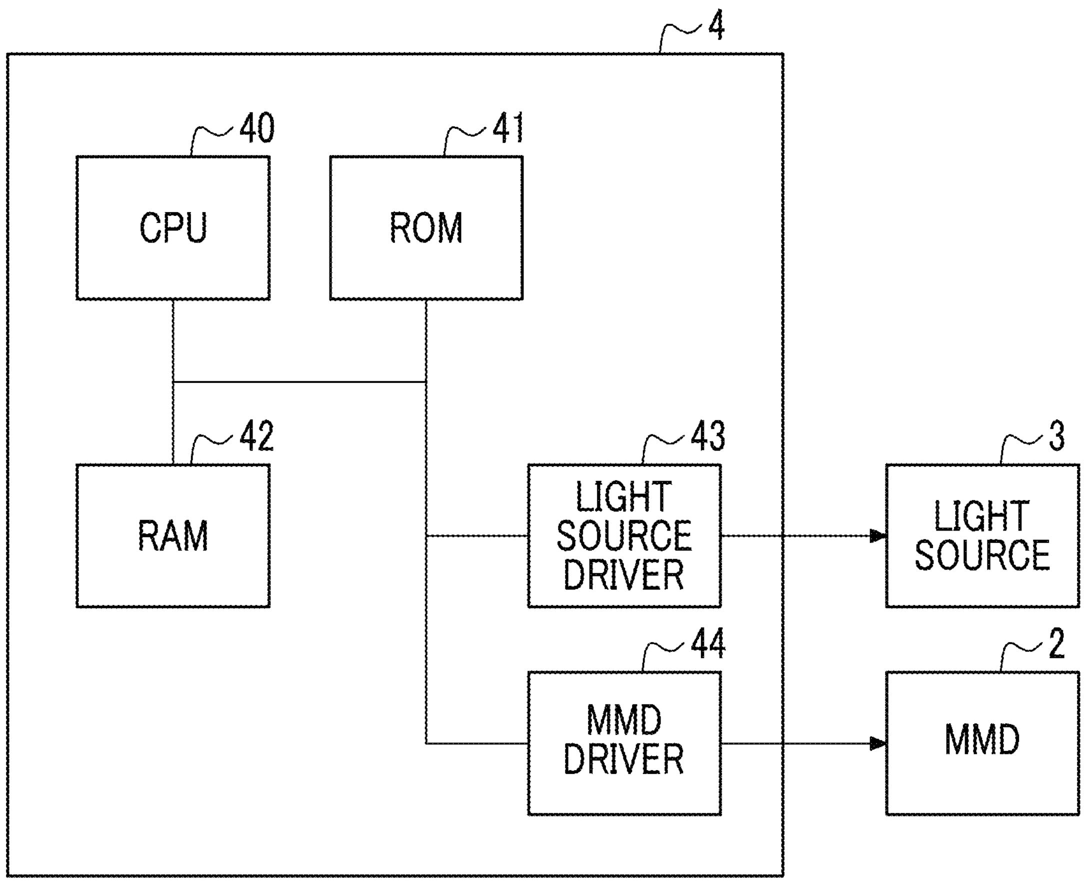
4
40
CPU
41
ROM
42
RAM
43
LIGHT SOURCE DRIVER
3
LIGHT SOURCE
44
MMD DRIVER
2
MMD

FIG. 3

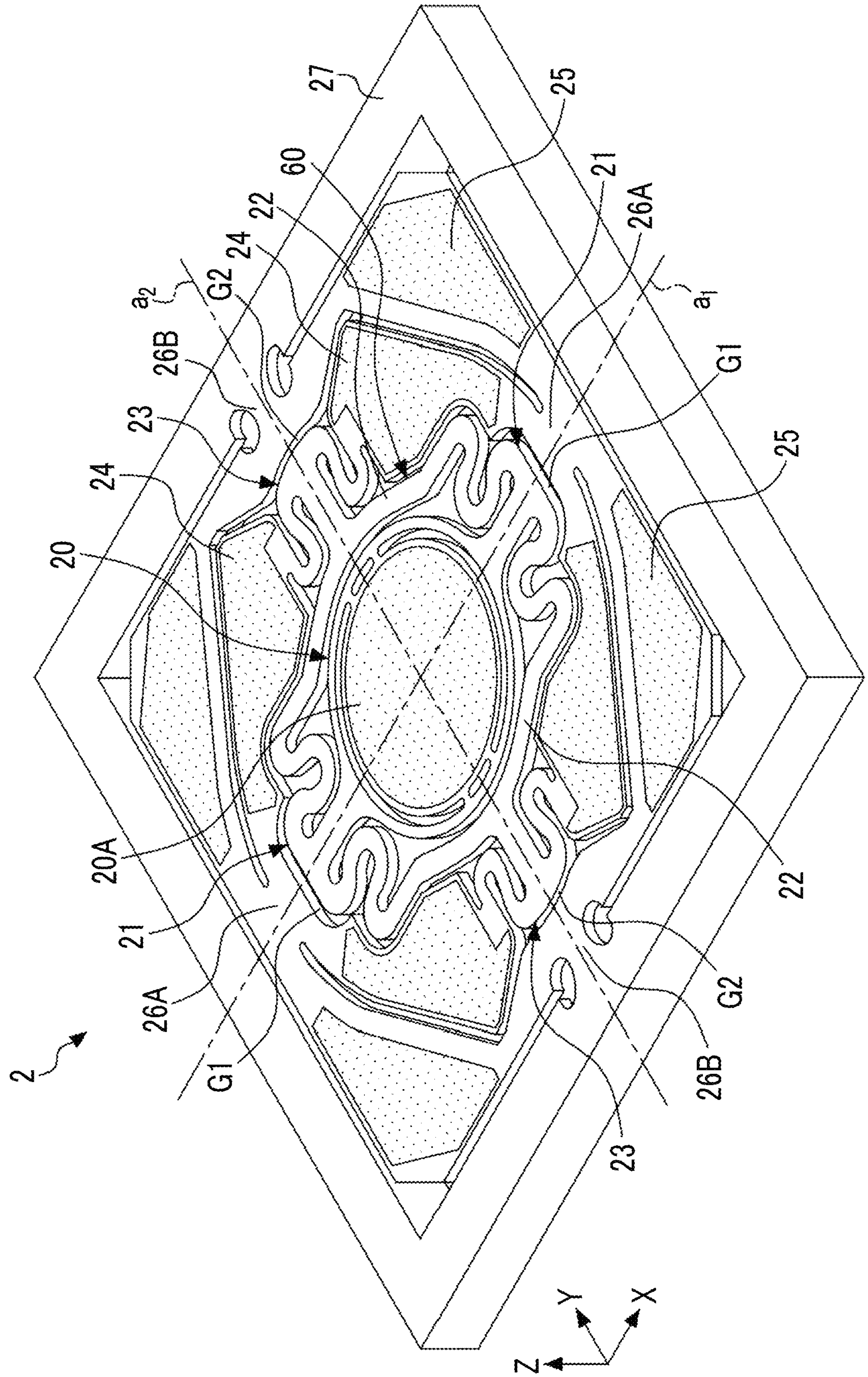
27
25
60
22
24
G2
a_2
26B
23
24
20
21
26A
a_1
G1
25
20A
21
26A
G1
2
22
G2
26B
23
Y
X
Z

FIG. 4

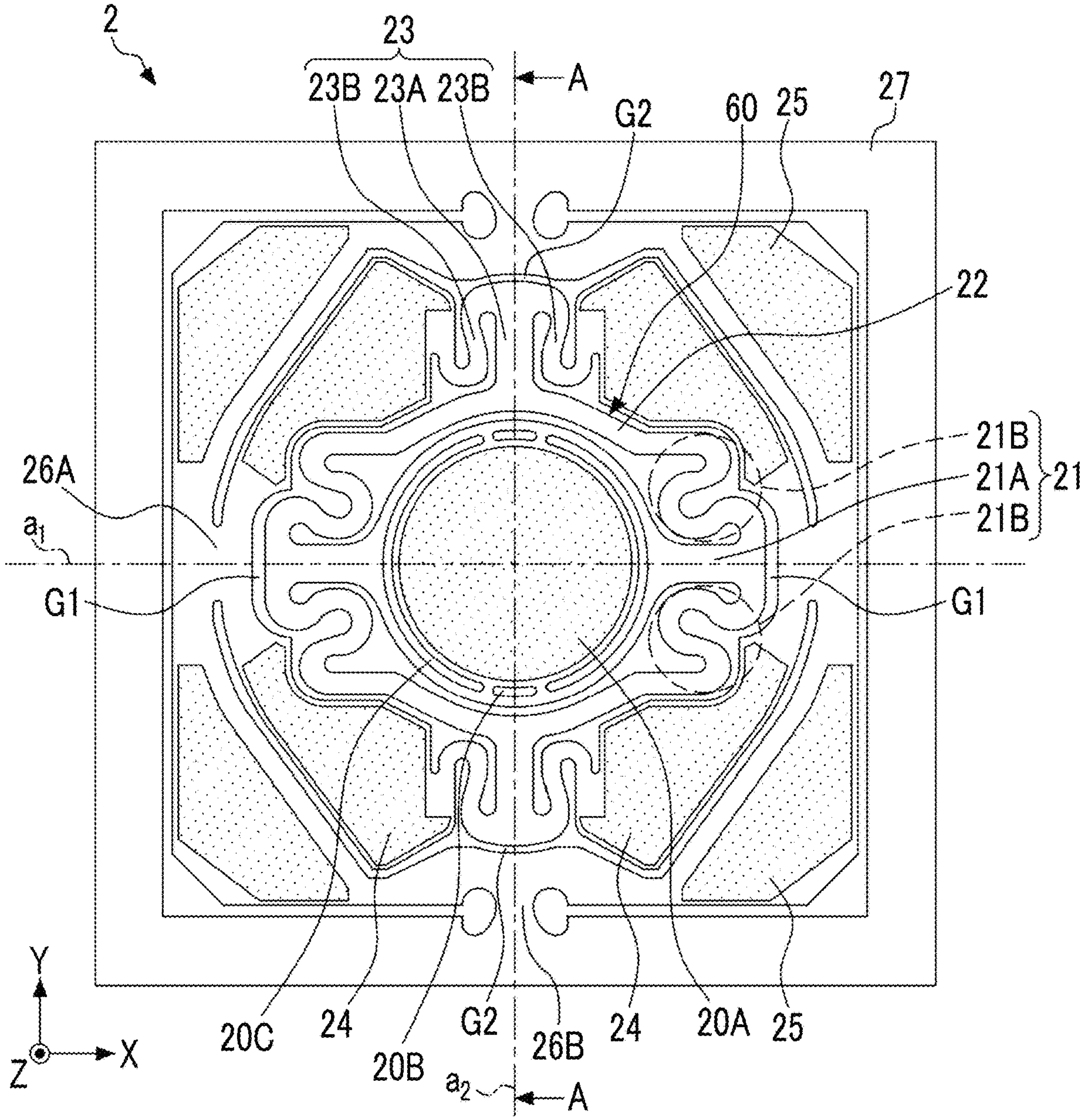
2
23
23B 23A 23B
A
G2
60
25
27
22
21B
21A
21
21B
26A
a_1
G1
G1
Y
X
Z
20C
24
20B
G2
26B
24
20A
25
a_2
A

FIG. 5

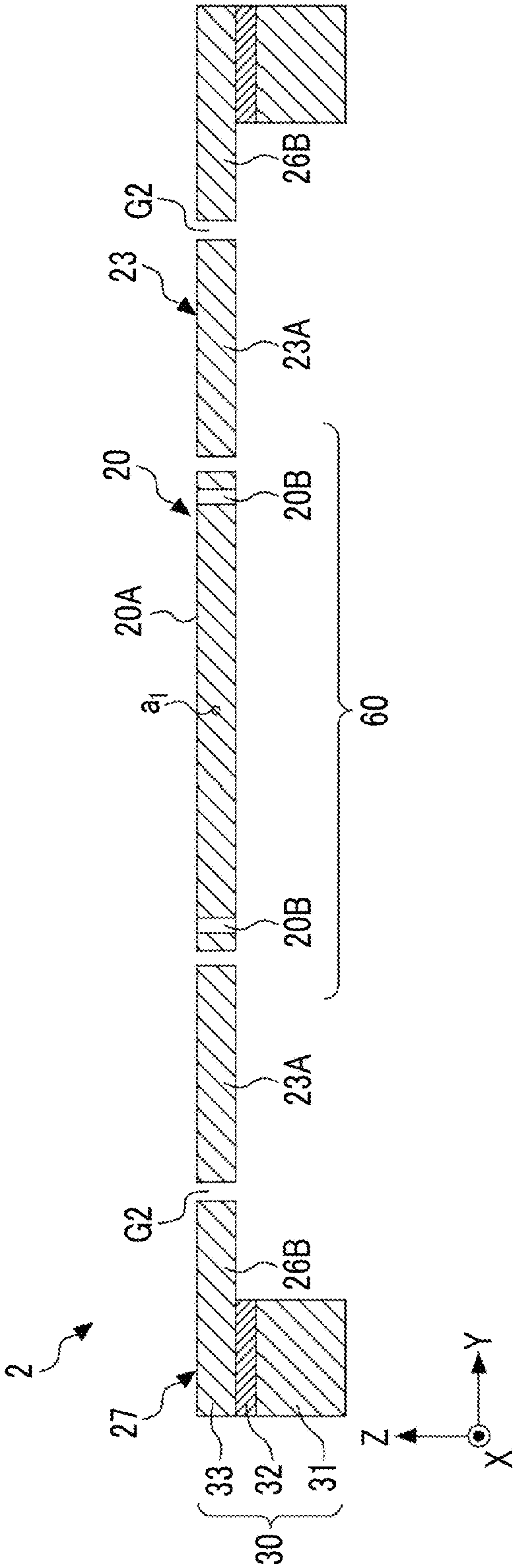

FIG. 6

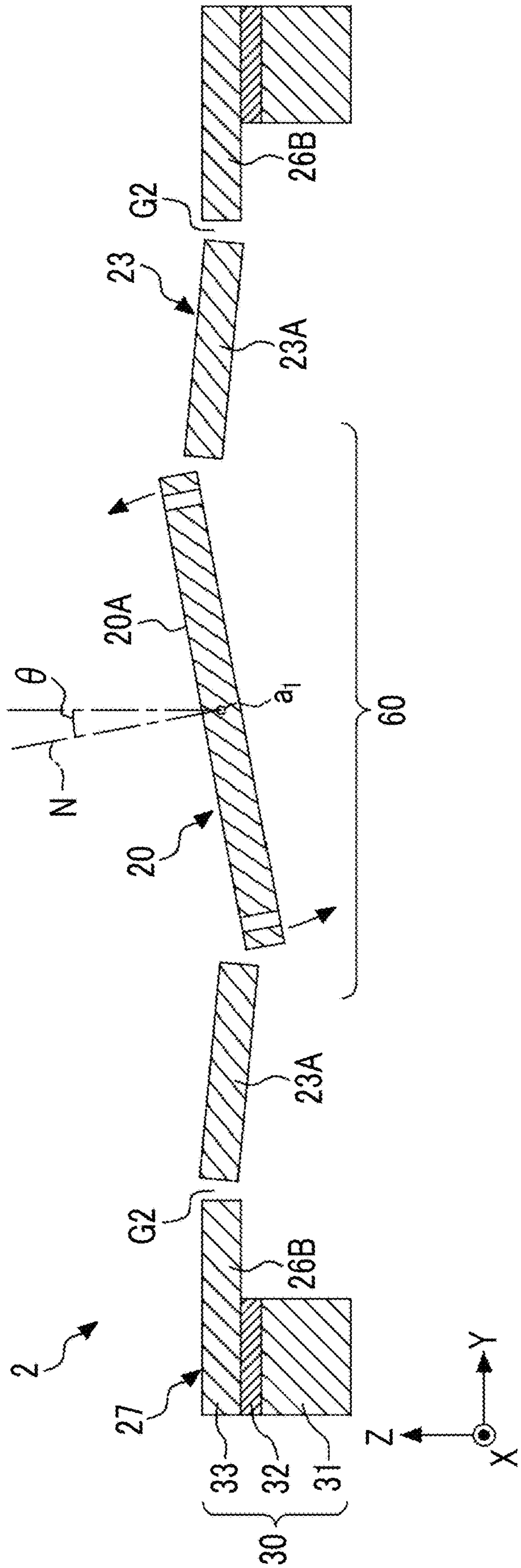

FIG. 7A

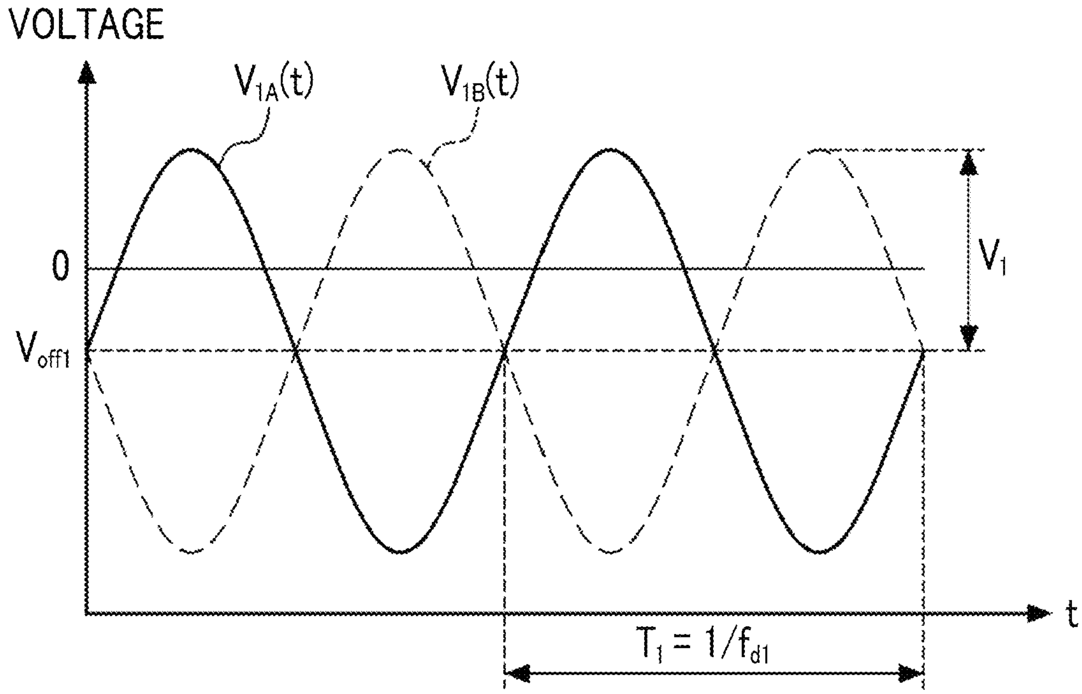
VOLTAGE
$V_{1A}(t)$
$V_{1B}(t)$
0
V_{off1}
V_1
t
$T_1 = 1/f_{d1}$

FIG. 7B

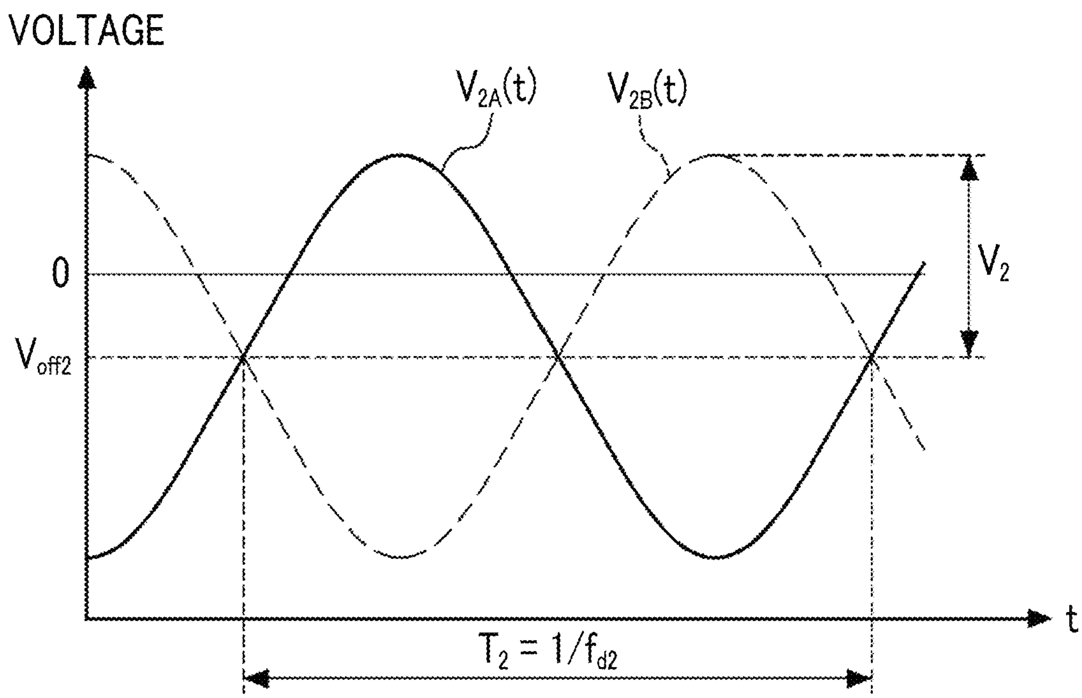
VOLTAGE
$V_{2A}(t)$
$V_{2B}(t)$
0
V_{off2}
V_2
t
$T_2 = 1/f_{d2}$

FIG. 8

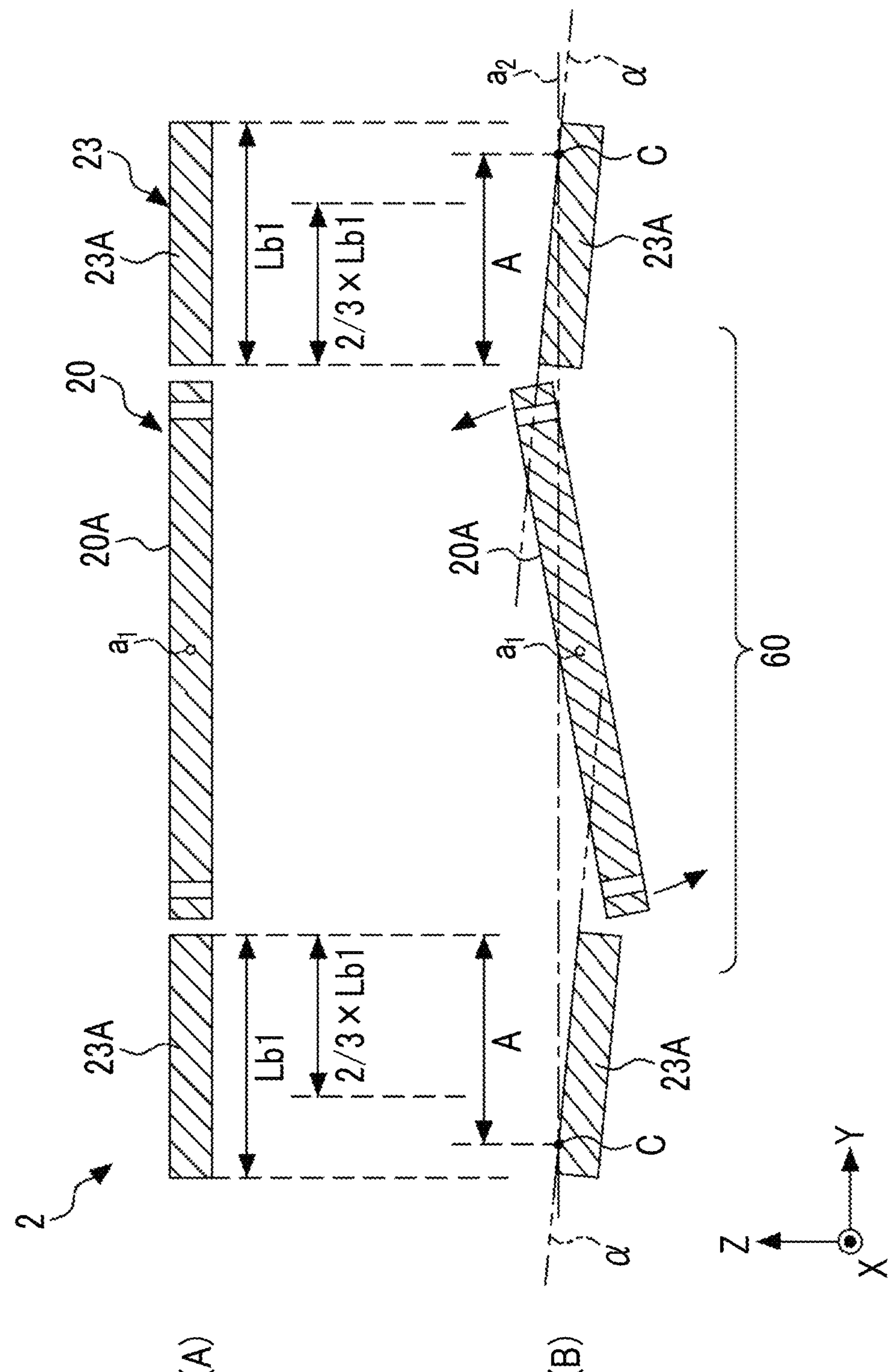

FIG. 9

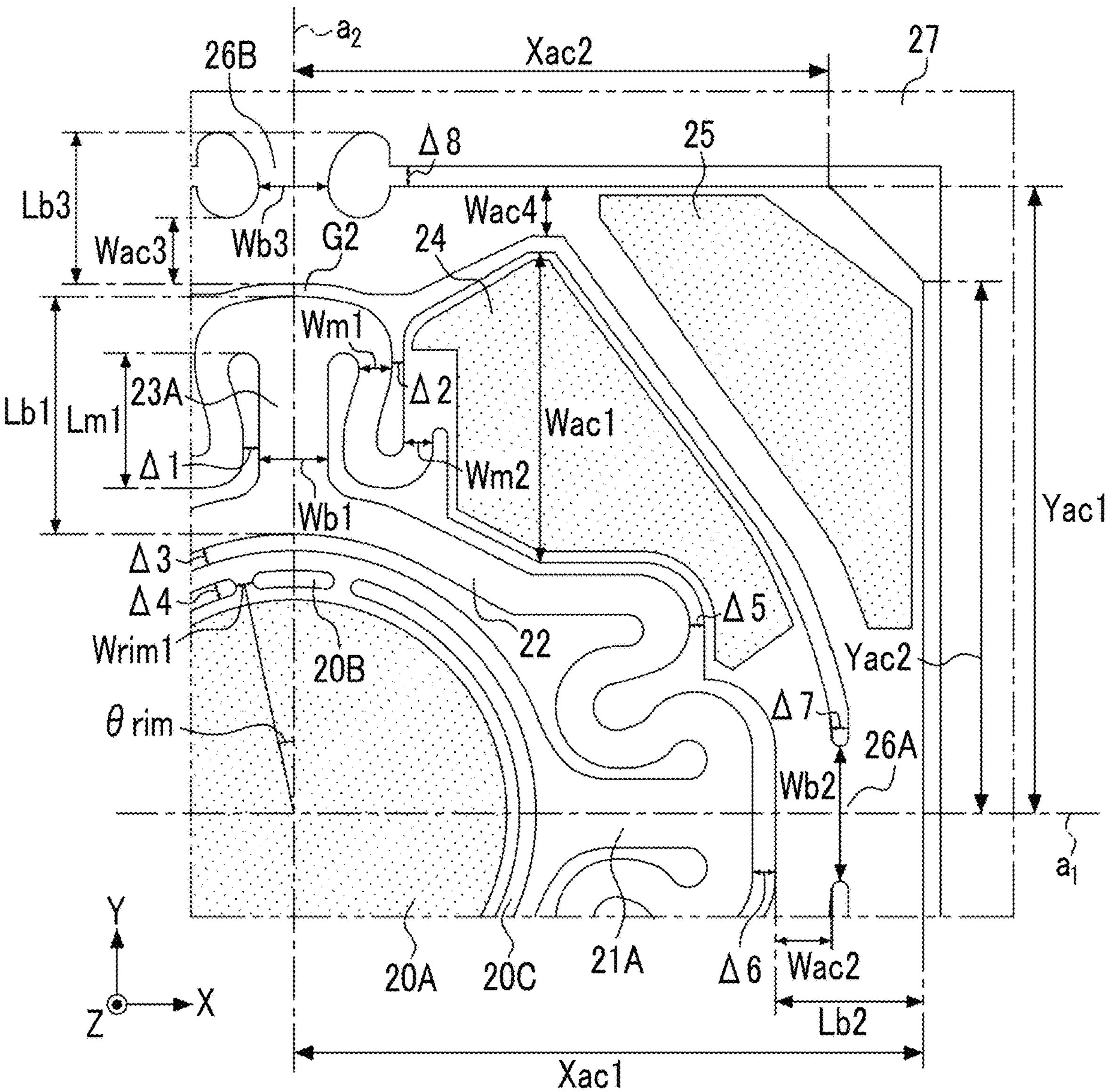

a2
26B
Xac2
27
Δ8
25
Lb3
Wac4
Wac3
Wb3
G2
24
Wm1
Lb1
23A
Δ2
Lm1
Wac1
Δ1
Wm2
Wb1
Yac1
Δ3
Δ5
Δ4
Wrim1
22
20B
Yac2
θ rim
Δ7
26A
Wb2
a1
Y
X
Z
20A
20C
21A
Δ6
Wac2
Lb2
Xac1

FIG. 10

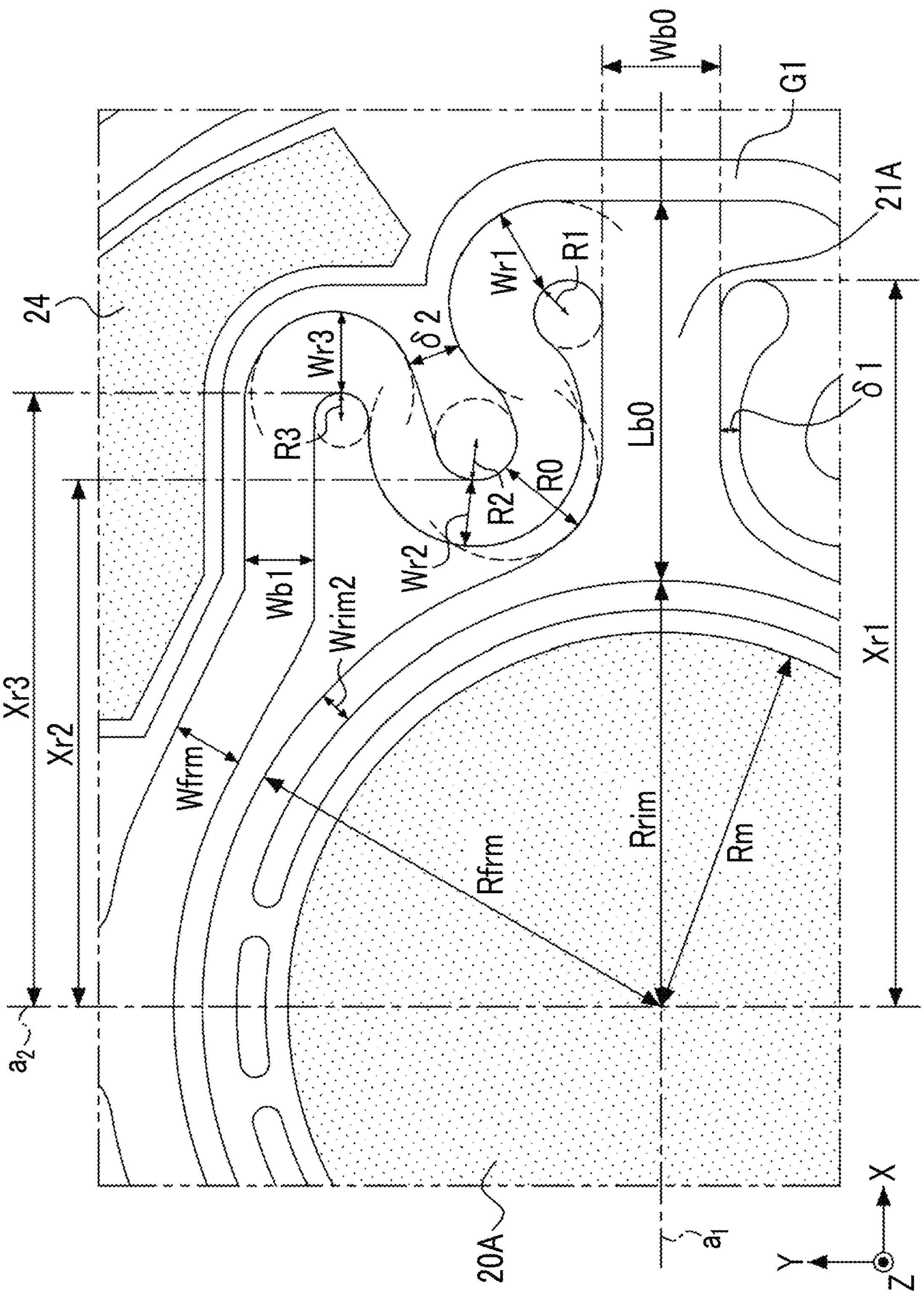
Wb0
G1
21A
R1
Wr1
24
δ2
Wr3
δ1
Lb0
R3
R0
R2
Wr2
Wb1
Wrim2
Xr3
Xr2
Xr1
Wfrm
Rrim
Rm
Rfrm
a2
a1
20A
X
Y
Z

FIG. 11

PARAMETER	SET VALUE
Lb1	0.790 mm
Wb1	0.230 mm
Lm1	0.450 mm
Lb2	0.490 mm
Wb2	0.425 mm
Lb3	0.500 mm
Wb3	0.215 mm
Wm1	0.110 mm
Wm2	0.100 mm
$\Delta 1$	0.050 mm
$\Delta 2$	0.040 mm
$\Delta 3$	0.050 mm
$\Delta 4$	0.050 mm
$\Delta 5$	0.060 mm
$\Delta 6$	0.070 mm
$\Delta 7$	0.050 mm
$\Delta 8$	0.065 mm
Wac1	1.030 mm
Wac2	0.190 mm
Wac3	0.220 mm
Wac4	0.170 mm
Xac1	2.090 mm
Xac2	VARIABLE
Yac1	2.090 mm
Yac2	VARIABLE
Wrim1	0.053 mm
θ rim	15.5°

PARAMETER	SET VALUE
Rm	0.750 mm
Lb0	0.730 mm
Wb0	0.220 mm
R0	0.230 mm
R1	0.065 mm
R2	0.075 mm
R3	0.050 mm
$\delta 1$	0.040 mm
$\delta 2$	0.095 mm
Wr1	0.165 mm
Wr2	0.125 mm
Wr3	0.148 mm
Xr1	1.376 mm
Xr2	0.990 mm
Xr3	1.159 mm
Wb1	0.132 mm
Wrim2	0.070 mm
Wfrm	0.136 mm
Rrim	0.800 mm
Rfrm	0.870 mm

FIG. 12

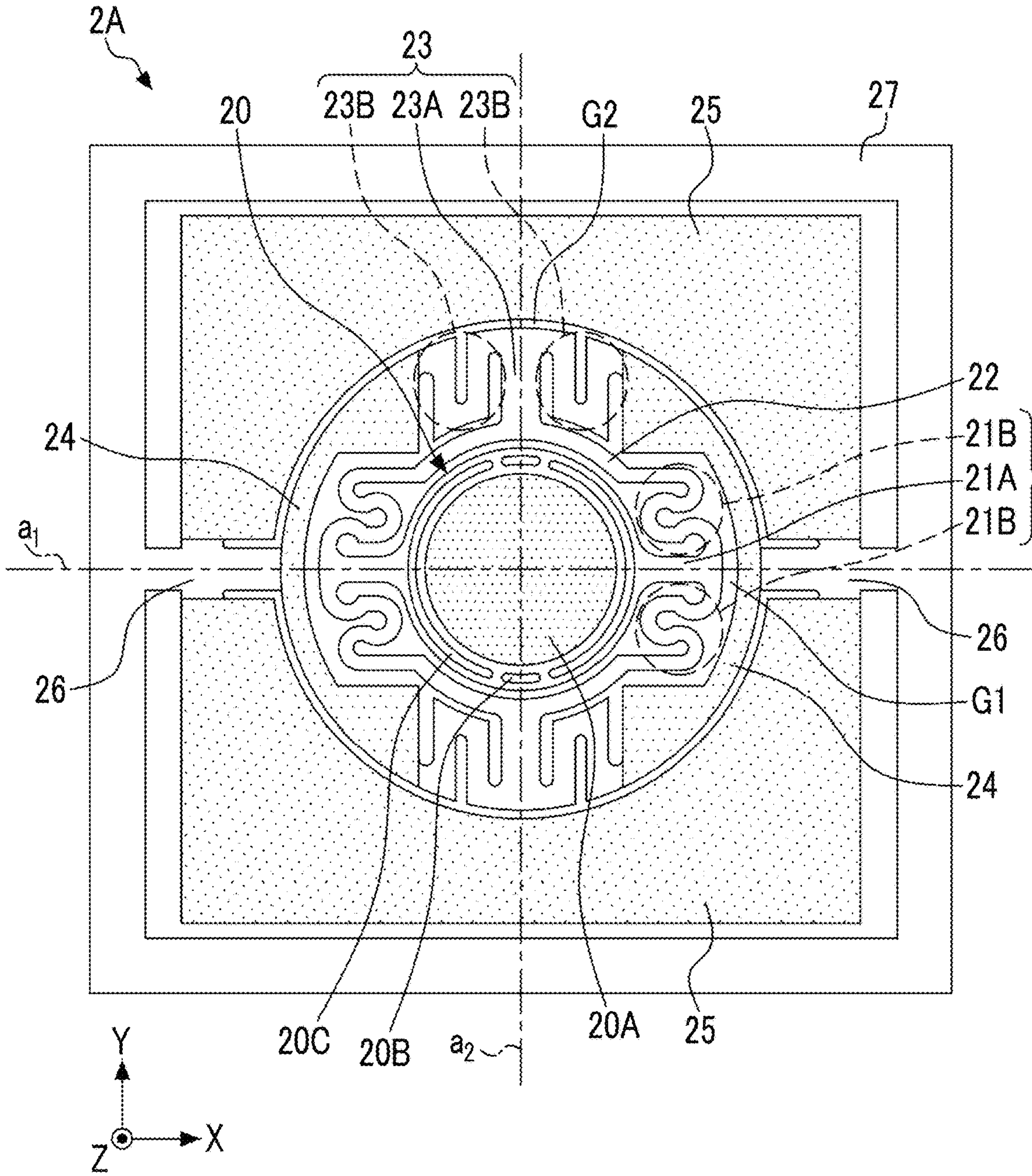

2A
23
23B
23A
23B
20
G2
25
27
22
21B
21A
21
21B
24
a_1
26
26
G1
24
20C
20B
a_2
20A
25
Y
X
Z

FIG. 13

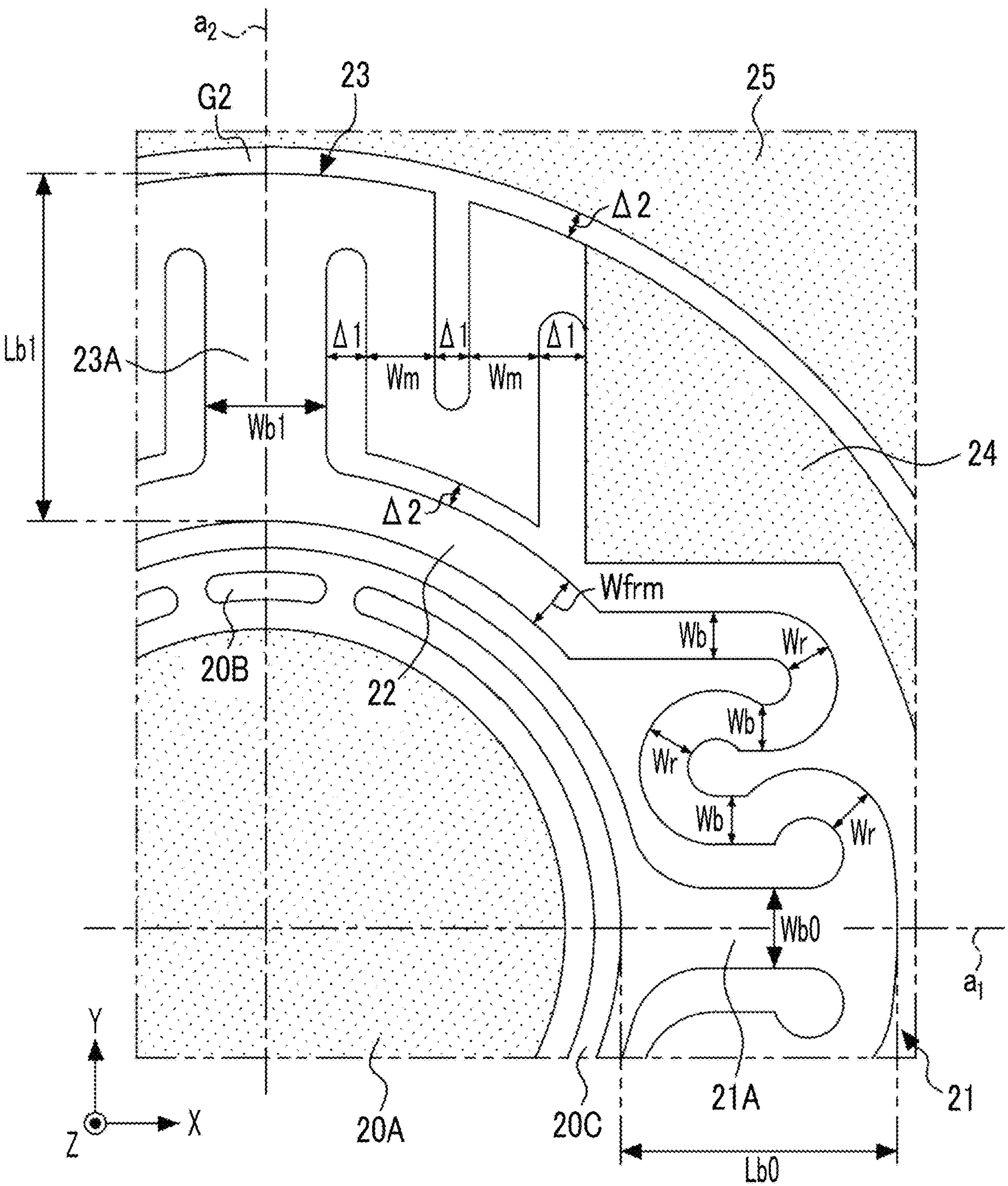

a2
G2
23
25
Δ2
Lb1
23A
Δ1
Δ1
Δ1
Wm
Wm
Wb1
24
Δ2
Wfrm
Wb
Wr
20B
22
Wb
Wr
Wb
Wr
Wb0
a1
Y
Z
X
20A
20C
21A
21
Lb0

FIG. 14

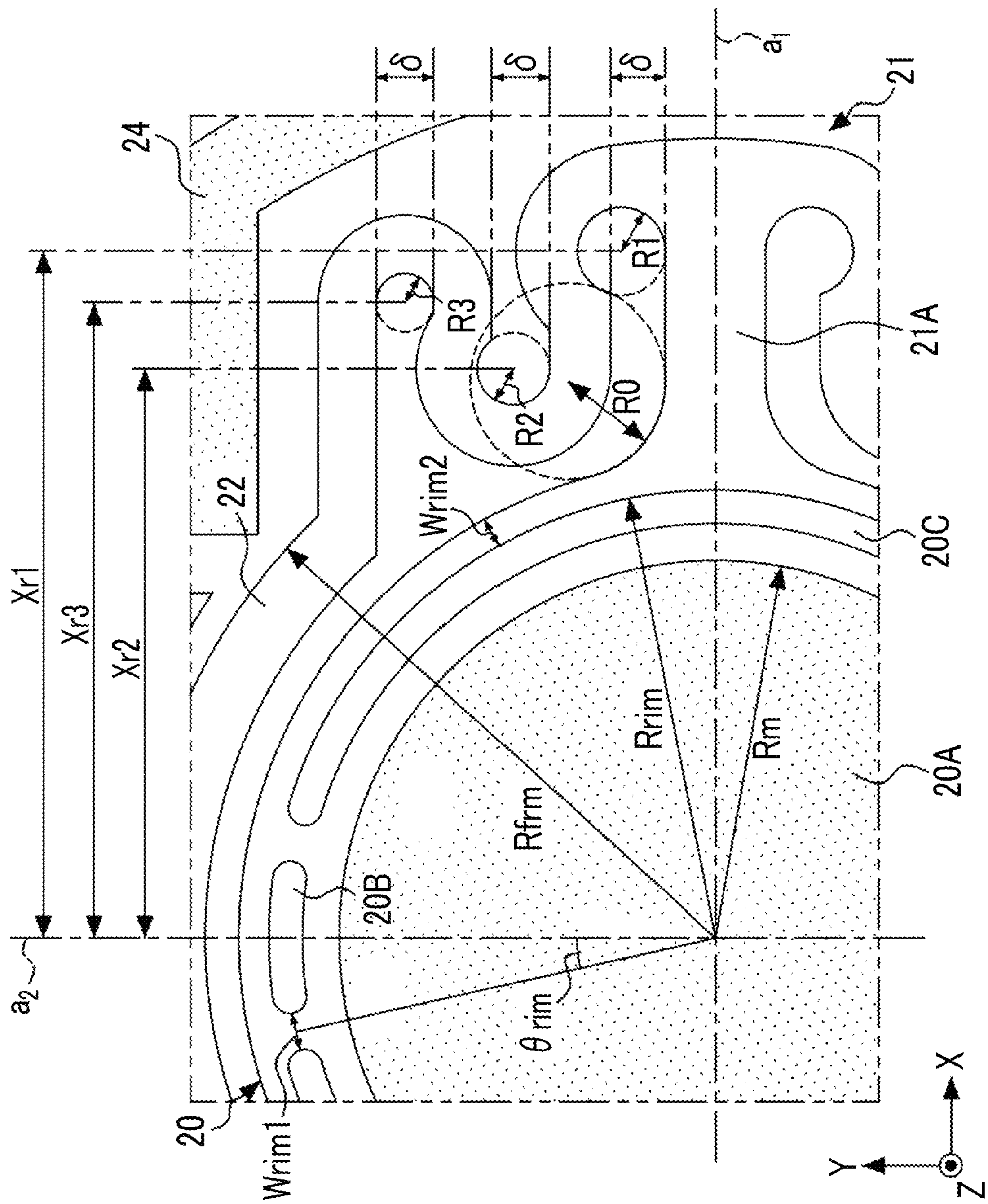
Xr1
Xr3
Xr2
a2
a1
δ
δ
δ
24
21
R1
R3
21A
R2
R0
22
Wrim2
20C
Rrim
Rm
Rfrm
20A
20B
θ rim
20
Wrim1
X
Y
Z

FIG. 15

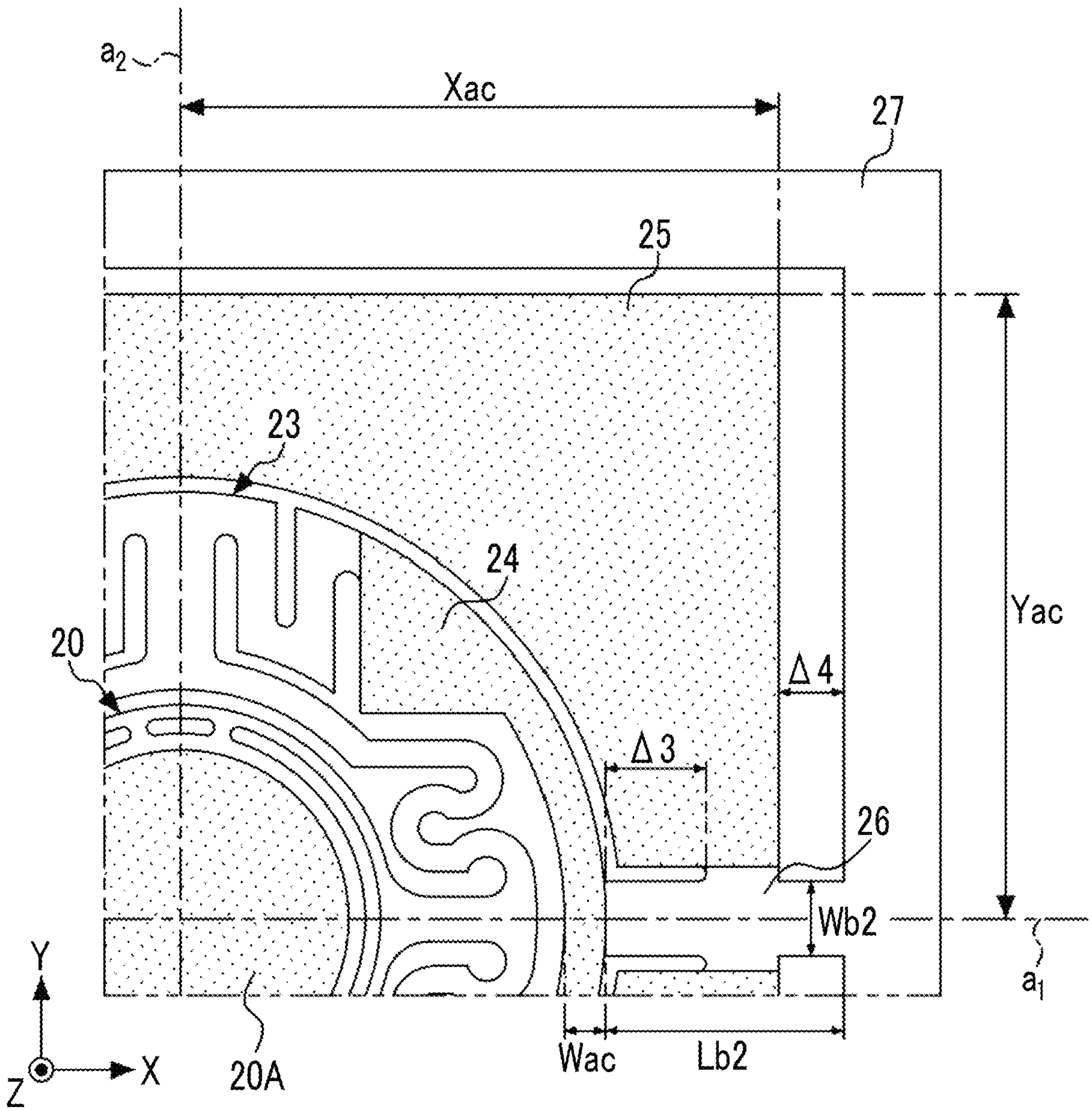

FIG. 16

PARAMETER	SET VALUE
Lb1	0.800 mm
Wb1	0.280 mm
Lb2	0.950 mm
Wb2	0.300 mm
Wm	0.16 mm
Δ1	0.085 mm
Δ2	0.050 mm
Δ3	0.400 mm
Δ4	0.250 mm
Wac	0.160 mm
Xac	2.415 mm
Yac	2.515 mm
Wrim1	0.05935 mm
θrim	12.5°

PARAMETER	SET VALUE
Rm	0.750 mm
Lb0	0.63825 mm
Wb0	0.185 mm
R0	0.17608 mm
R1	0.065 mm
R2	0.075 mm
R3	0.050 mm
δ	0.090 mm
Wb	0.120 mm
Wr	0.120 mm
Xr1	1.23191 mm
Xr2	1.02796 mm
Xr3	1.14471 mm
Wrim2	0.065 mm
Rrim	0.800 mm
Wfrm	0.130 mm
Rfrm	1.045 mm

FIG. 17

SAMPLE NUMBER	Xac2 (mm)	Yac2 (mm)	Lb1 (mm)	A (mm)	A/Lb1	fr1 (Hz)	fr2 (Hz)	Δfr (Hz)	STABILITY OF TWO-DIMENSIONAL DRIVING	POWER CONSUMPTION (mW)
1	–	–	0.80	0.16	0.20	34427	34257	−170	NG	3
2	1.39	1.44	0.79	0.23	0.30	29237	29118	−119	NG	9
3	1.57	1.79	0.79	0.43	0.54	28740	28679	−61	NG	30
4	1.66	1.83	0.79	0.52	0.66	28517	28467	−50	OK	41
5	1.75	1.87	0.79	0.61	0.77	28294	28252	−42	OK	52
6	1.84	1.90	0.79	0.70	0.89	28125	28089	−36	OK	60
7	1.97	1.94	0.79	0.78	0.99	27995	27964	−31	OK	66
8	2.03	2.02	0.79	0.88	1.11	27522	27495	−27	OK	75
9	2.09	2.09	0.79	0.97	1.23	27480	27458	−22	OK	82

FIG. 18

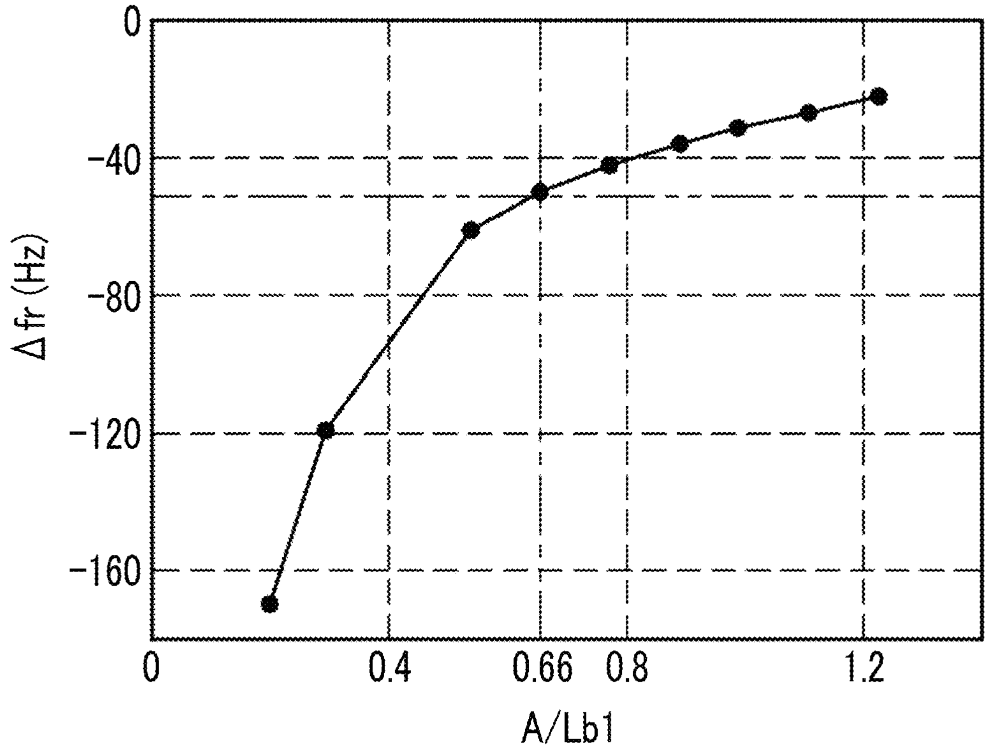
0
-40
-80
-120
-160
Δ fr (Hz)
0
0.4
0.66
0.8
1.2
A/Lb1

FIG. 19

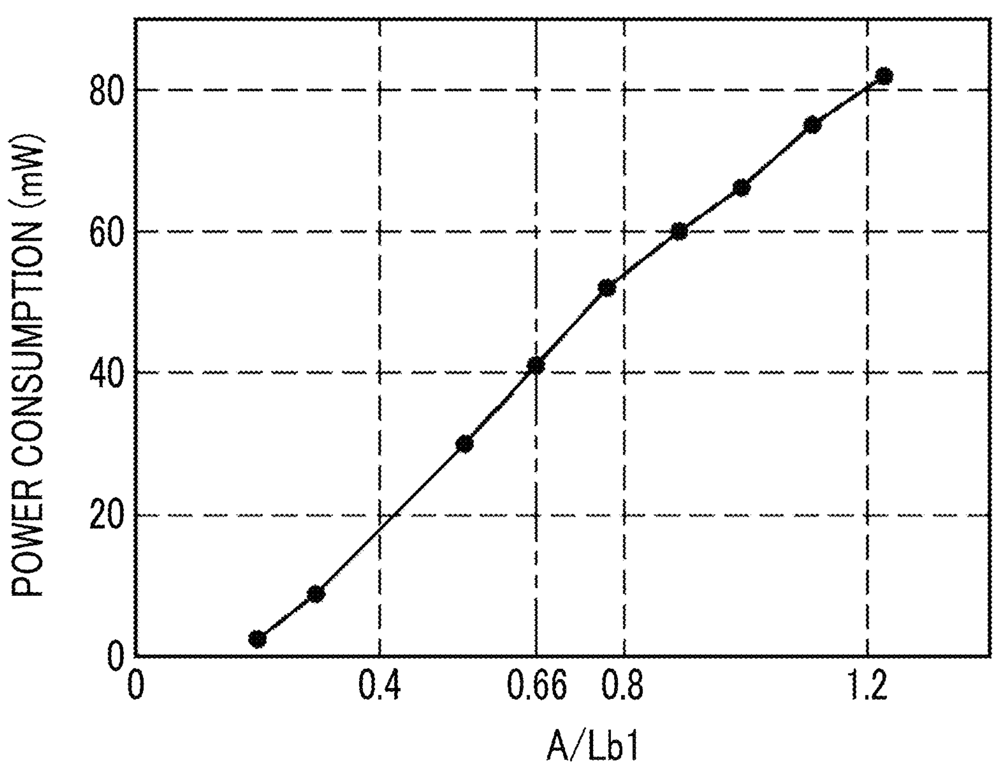
80
60
40
20
0
POWER CONSUMPTION (mW)
0
0.4
0.66
0.8
1.2
A/Lb1

FIG. 20

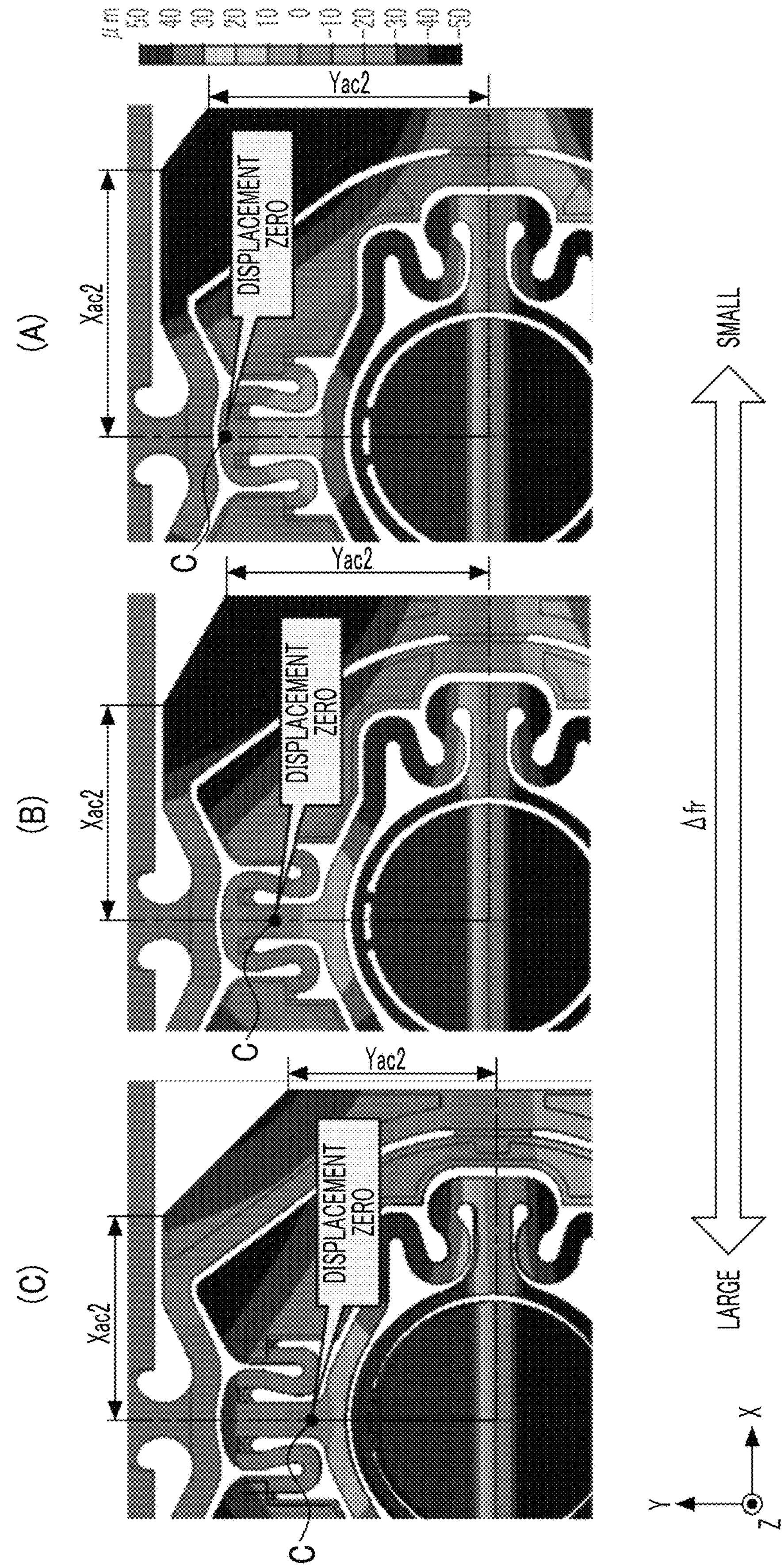
μm
50
40
30
20
10
0
−10
−20
−30
−40
−50
(A)
(B)
(C)
Xac2
Yac2
DISPLACEMENT ZERO
C
SMALL
Δfr
LARGE
X
Y
Z

MICROMIRROR DEVICE AND OPTICAL SCANNING DEVICE

CROSS-REFERENCE TO RELATED APPLICATIONS

The present application claims priority under 35 U.S.C. § 119 to Japanese Patent Application No. 2021-146275 filed on Sep. 8, 2021. The above application is hereby expressly incorporated by reference, in its entirety, into the present application.

BACKGROUND

1. Technical Field

The technique of the present disclosure relates to a micromirror device and an optical scanning device.

2. Description of the Related Art

A micromirror device (also referred to as a microscanner) is known as one of micro electro mechanical systems (MEMS) devices manufactured using the silicon (Si) microfabrication technique. Since the micromirror device is small and has low power consumption, it is expected to have a wide range of applications in laser displays, laser projectors, optical coherence tomography, and the like.

There are various drive methods for the micromirror device, and a piezoelectric drive method using deformation of a piezoelectric body is promising since the generated torque is higher than that in other methods and a high scan angle can be obtained. In particular, in a case where a high scan angle is required, such as in a laser display, a higher scan angle can be obtained by resonantly driving the micromirror device of the piezoelectric drive method.

A general micromirror device used in a laser display comprises a mirror portion and a piezoelectric actuator (see, for example, JP2017-132281A and WO2009/041342A). The mirror portion is swingable around a first axis and a second axis that are orthogonal to each other. The actuator allows the mirror portion to swing around the first axis and the second axis according to the driving voltage supplied from the outside. The above-described scan angle corresponds to a deflection angle of the mirror portion.

As performance indicators of the laser display, resolution and viewing angle are mentioned. The resolution and viewing angle are related to a swing frequency and a deflection angle of the mirror portion of the micromirror device. For example, in a laser display of a Lissajous scanning method, two-dimensional optical scanning is performed by allowing the mirror portion to swing sequentially at two different frequencies around the first axis and the second axis. The larger the deflection angle of the mirror portion, the larger the scanning area of light, and the larger the image can be displayed with the shorter optical path length.

SUMMARY

Generally, in a case where the micromirror device is driven resonantly, a crosstalk between axes is generated in which the swing of the mirror portion around one of the first axis and the second axis affects the swing of the mirror portion around the other axis. Specifically, according to the size of a rotation angle around the one axis, a resonance

frequency around the other axis shifts. As a result, the stability of the two-dimensional optical scanning is significantly reduced.

For example, in a case where a driving frequency around the one axis is swept to bring the driving frequency closer to the resonance frequency to increase a deflection angle of the mirror portion, a deflection angle of the mirror portion around the other axis is greatly changed by the shift of the resonance frequency caused by the crosstalk between axes. In this case, a change in the deflection angle of the mirror portion around the other axis causes a shift of the resonance frequency around the axis on a side where the driving frequency is swept. That is, the crosstalk between axes causes a kind of feedback phenomenon.

In this way, in a case where a shift amount of the resonance frequency by the crosstalk between axes is large, even though the driving frequency is swept, there are problems that the driving frequency cannot be adjusted to the resonance frequency due to the feedback phenomenon, and that the deflection angle of the mirror portion cannot be increased.

An object of the present disclosure is to provide a micromirror device and an optical scanning device capable of suppressing a shift of a resonance frequency by a crosstalk between axes.

In order to achieve the object, a micromirror device of the present disclosure comprises: a mirror portion on which a reflecting surface for reflecting incident light is formed; a first support portion that is connected to the mirror portion on a first axis located in a plane including the reflecting surface of the mirror portion in a stationary state, and that swingably supports the mirror portion around the first axis; a pair of movable frames that are connected to the first support portion and face each other across the first axis; a second support portion that is connected to the movable frame on a second axis which is located in the plane including the reflecting surface of the mirror portion in the stationary state and is orthogonal to the first axis, and that swingably supports a movable portion including the mirror portion, the first support portion, and the movable frame around the second axis; a driving portion that surrounds the movable portion and has a gap with the second support portion on the second axis; a coupling portion that couples the second support portion and the driving portion; and a fixed frame that is connected to the driving portion and surrounds the driving portion, in which, in a state where the mirror portion rotates around the first axis and an absolute value of a rotation angle is larger than 0 degrees, assuming that, in a plane orthogonal to the first axis and including the second axis, a distance between an intersection between the second axis and a straight line located on a surface of the second support portion and including each end point of the second support portion and an end part of the second support portion on a mirror portion side in the stationary state is denoted by A, and a total length of the second support portion in a direction of the second axis is denoted by L, a relationship of $2/3 < A/L$ is satisfied.

It is preferable that the driving portion has a piezoelectric element.

It is preferable that the driving portion includes a pair of first actuators facing each other across the second axis and having a piezoelectric element, and a pair of second actuators surrounding the first actuator, facing each other across the first axis, and having a piezoelectric element.

It is preferable that the second actuator allows the mirror portion to swing around the first axis, and the first actuator allows the movable portion to swing around the second axis.

It is preferable that the distance A and the total length L satisfy a relationship of $2/3<A/L<6/5$.

An optical scanning device of the present disclosure comprises: the micromirror device according to any one of the aspects; and a processor that drives the driving portion, in which the processor allows the mirror portion to swing around the first axis and the second axis by providing a driving signal to the driving portion.

According to the technique of the present disclosure, it is possible to provide a micromirror device and an optical scanning device capable of suppressing a shift of a resonance frequency by a crosstalk between axes.

BRIEF DESCRIPTION OF THE DRAWINGS

Exemplary embodiments according to the technique of the present disclosure will be described in detail based on the following figures, wherein:

FIG. **1** is a schematic view of an optical scanning device,

FIG. **2** is a block diagram showing an example of a hardware configuration of a driving controller,

FIG. **3** is an external perspective view of a micromirror device,

FIG. **4** is a plan view of the micromirror device as viewed from a light incident side,

FIG. **5** is a cross-sectional view taken along the line A-A of FIG. **4**,

FIG. **6** is a cross-sectional view showing a state where a mirror portion rotates around a first axis,

FIGS. **7**A and **7**B are diagrams showing examples of a first driving signal and a second driving signal,

FIG. **8** is a diagram schematically showing displacement of a second support portion in a case where the mirror portion rotates around the first axis,

FIG. **9** is a diagram showing parameters relating to dimensions of components of the micromirror device,

FIG. **10** is a diagram showing parameters relating to dimensions of components of the micromirror device,

FIG. **11** is a diagram showing specific setting values of the parameters,

FIG. **12** is a plan view of a micromirror device according to Modification Example,

FIG. **13** is a diagram showing parameters relating to dimensions of components of the micromirror device according to Modification Example,

FIG. **14** is a diagram showing parameters relating to dimensions of components of the micromirror device according to Modification Example,

FIG. **15** is a diagram showing parameters relating to dimensions of components of the micromirror device according to Modification Example,

FIG. **16** is a diagram showing specific setting values of the parameters,

FIG. **17** is a diagram showing experimental results for each sample,

FIG. **18** is a graph showing dependence of a shift amount of a resonance frequency on a ratio A/Lb**1**,

FIG. **19** is a graph showing dependence of power consumption on the ratio A/Lb**1**, and

FIG. **20** is a diagram showing simulation results.

DETAILED DESCRIPTION

An example of an embodiment relating to the technique of the present disclosure will be described with reference to the accompanying drawings.

FIG. **1** schematically shows an optical scanning device **10** according to an embodiment. The optical scanning device **10** includes a micromirror device (hereinafter, referred to as micromirror device (MMD)) **2**, a light source **3**, and a driving controller **4**. The optical scanning device **10** optically scans a surface to be scanned **5** by reflecting a light beam L emitted from the light source **3** by the MMD **2** under the control of the driving controller **4**. The surface to be scanned **5** is, for example, a screen.

The MMD **2** is a piezoelectric biaxial drive type micromirror device capable of allowing a mirror portion **20** (see FIG. **3**) to swing around a first axis a_1 and a second axis a_2 orthogonal to the first axis a_1. Hereinafter, the direction parallel to the first axis a_1 is referred to as an X direction, the direction parallel to the second axis a_2 is a Y direction, and the direction orthogonal to the first axis a_1 and the second axis a_2 is referred to as a Z direction.

The light source **3** is a laser device that emits, for example, laser light as the light beam L. It is preferable that the light source **3** emits the light beam L perpendicularly to a reflecting surface **20**A (see FIG. **3**) included in the mirror portion **20** in a state where the mirror portion **20** of the MMD **2** is stationary.

The driving controller **4** outputs a driving signal to the light source **3** and the MMD **2** based on optical scanning information. The light source **3** generates the light beam L based on the input driving signal and emits the light beam L to the MMD **2**. The MMD **2** allows the mirror portion **20** to swing around the first axis a_1 and the second axis a_2 based on the input driving signal.

As will be described in detail below, the driving controller **4** allows the mirror portion **20** to resonate around the first axis a_1 and the second axis a_2, so that the surface to be scanned **5** is scanned with the light beam L reflected by the mirror portion **20** such that a Lissajous waveform is drawn. This optical scanning method is called a Lissajous scanning method.

The optical scanning device **10** is applied to, for example, a Lissajous scanning type laser display. Specifically, the optical scanning device **10** can be applied to a laser scanning display such as augmented reality (AR) glass or virtual reality (VR) glass.

FIG. **2** shows an example of a hardware configuration of the driving controller **4**. The driving controller **4** has a central processing unit (CPU) **40**, a read only memory (ROM) **41**, a random access memory (RAM) **42**, a light source driver **43**, and an MMD driver **44**. The CPU **40** is an arithmetic unit that realizes the entire function of the driving controller **4** by reading out a program and data from a storage device such as the ROM **41** into the RAM **42** and executing processing. The CPU **40** is an example of a "processor" according to the technique of the present disclosure.

The ROM **41** is a non-volatile storage device and stores a program for the CPU **40** to execute processing and data such as the optical scanning information described above. The RAM **42** is a volatile storage device that temporarily holds a program and data.

The light source driver **43** is an electric circuit that outputs a driving signal to the light source **3** under the control of the CPU **40**. In the light source driver **43**, the driving signal is a driving voltage for controlling the irradiation timing and the irradiation intensity of the light source **3**.

The MMD driver **44** is an electric circuit that outputs a driving signal to the MMD **2** under the control of the CPU **40**. In the MMD driver **44**, the driving signal is a driving voltage for controlling the timing, cycle, and deflection angle for allowing the mirror portion **20** of the MMD **2** to swing.

The CPU **40** controls the light source driver **43** and the MMD driver **44** based on the optical scanning information. The optical scanning information is information including the scanning pattern of the light beam L with which the surface to be scanned **5** is scanned and the light emission timing of the light source **3**.

Next, the configuration of the MMD **2** according to a first embodiment will be described with reference to FIGS. **3** to **5**. FIG. **3** is an external perspective view of the MMD **2**. FIG. **4** is a plan view of the MMD **2** as viewed from the light incident side. FIG. **5** is a cross-sectional view taken along the line A-A in FIG. **4**.

As shown in FIG. **3**, the MMD **2** has the mirror portion **20**, a pair of first support portions **21**, a pair of movable frames **22**, a pair of second support portions **23**, a pair of first actuators **24**, a pair of second actuators **25**, a pair of first connecting portions **26**A, a pair of second connecting portions **26**B, and a fixed frame **27**. The MMD **2** is a so-called MEMS scanner.

The mirror portion **20** has a reflecting surface **20**A for reflecting incident light. The reflecting surface **20**A is formed of a metal thin film such as gold (Au) and aluminum (Al) provided on one surface of the mirror portion **20**. The shape of the reflecting surface **20**A is, for example, circular with the intersection of the first axis a_1 and the second axis a_2 as the center.

The first axis a_1 and the second axis a_2 exist, for example, in a plane including the reflecting surface **20**A in a case where the mirror portion **20** is stationary. The planar shape of the MMD **2** is rectangular, line-symmetrical with respect to the first axis a_1, and line-symmetrical with respect to the second axis a_2.

The pair of first support portions **21** are disposed at positions facing each other across the second axis a_2, and have a shape that is line-symmetrical with respect to the second axis a_2. In addition, each of the first support portions **21** has a shape that is line-symmetrical with respect to the first axis a_1. The first support portion **21** is connected to the mirror portion **20** on the first axis a_1, and swingably supports the mirror portion **20** around the first axis a_1.

The pair of movable frames **22** are disposed at positions facing each other across the first axis a_1, and have a shape that is line-symmetrical with respect to the first axis a_1. Each of the movable frames **22** has a shape that is line-symmetrical with respect to the second axis a_2. In addition, each of the movable frames **22** is curved along the outer periphery of the mirror portion **20**. Both ends of the movable frame **22** are connected to the first support portion **21**.

The first support portion **21** and the movable frame **22** are connected to each other to surround the mirror portion **20**. The mirror portion **20**, the first support portion **21**, and the movable frame **22** constitute the movable portion **60**.

The pair of second support portions **23** are disposed at positions facing each other across the first axis a_1, and have a shape that is line-symmetrical with respect to the first axis a_1. Each of the second support portions **23** has a shape that is line-symmetrical with respect to the second axis a_2. The second support portion **23** is connected to the movable frame **22** on the second axis a_2, and swingably supports the movable portion **60** having the mirror portion **20** around the second axis a_2. In addition, both ends of the second support portion **23** are connected to the first actuator **24**.

The pair of first actuators **24** are disposed at positions facing each other across the second axis a_2, and have a shape that is line-symmetrical with respect to the second axis a_2. In addition, each of the first actuators **24** has a shape that is line-symmetrical with respect to the first axis a_1. The first actuator **24** is formed along the outer periphery of the movable frame **22** and the first support portion **21**. The first actuator **24** is a piezoelectric drive type actuator comprising a piezoelectric element.

In FIGS. **3** and **4**, although it seems that the first actuator **24** is divided in the vicinity of the first axis a_1, the first actuator **24** is electrically connected by a wiring line (not shown) via the first axis a_1.

The second support portion **23** and the first actuator **24** are connected to each other to surround the movable portion **60**.

The pair of second actuators **25** are disposed at positions facing each other across the first axis a_1, and have a shape that is line-symmetrical with respect to the first axis a_1. In addition, each of the second actuators **25** has a shape that is line-symmetrical with respect to the second axis a_2. The second actuator **25** is formed along the outer periphery of the first actuator **24** and the second support portion **23**. The second actuator **25** is a piezoelectric drive type actuator comprising a piezoelectric element.

In FIGS. **3** and **4**, although it seems that the second actuator **25** is divided in the vicinity of the second axis a_2, the second actuator **25** is electrically connected by a wiring line (not shown) via the second axis a_2.

The pair of first connecting portions **26**A are disposed at positions facing each other across the second axis a_2, and have a shape that is line-symmetrical with respect to the second axis a_2. In addition, each of the first connecting portions **26**A has a shape that is line-symmetrical with respect to the first axis a_1. The first connecting portion **26**A is disposed along the first axis a_1, and connects the first actuator **24** and the second actuator **25** on the first axis a_1.

The pair of second connecting portions **26**B are disposed at positions facing each other across the first axis a_1, and have a shape that is line-symmetrical with respect to the first axis a_1. In addition, each of the second connecting portions **26**B has a shape that is line-symmetrical with respect to the second axis a_2. The second connecting portion **26**B is disposed along the second axis a_2, and connects the second actuator **25** and the fixed frame **27** on the second axis a_2.

The second actuator **25** and the second connecting portion **26**B are connected to each other to surround the movable portion **60** and the first actuator **24**. The first actuator **24** and the second actuator **25** constitute a driving portion surrounding the movable portion **60**.

The fixed frame **27** is a frame-shaped member having a rectangular outer shape, and has a shape that is line-symmetrical with respect to each of the first axis a_1 and the second axis a_2. The fixed frame **27** surrounds the outer periphery of the second actuator **25** and the second connecting portion **26**B. That is, the fixed frame **27** surrounds the driving portion.

The first actuator **24** and the second actuator **25** are piezoelectric actuators each having a piezoelectric element. The pair of first actuators **24** allow the movable portion **60** to swing around the second axis a_2 by applying rotational torque around the second axis a_2 to the mirror portion **20** and the movable frame **22**. The pair of second actuators **25** allow the mirror portion **20** to swing around the first axis a_1 by applying rotational torque around the first axis a_1 to the mirror portion **20**, the movable frame **22**, and the first actuator **24**.

As shown in FIG. **4**, the first support portion **21** is composed of a swing shaft **21**A and a pair of coupling portions **21**B. The swing shaft **21**A is a so-called torsion bar stretched along the first axis a_1. One end of the swing shaft **21**A is connected to the mirror portion **20**, and the other end thereof is connected to the coupling portion **21**B.

On the first axis a_1, there is a spatial gap (hereinafter, referred to as a gap) G**1** between the first support portion **21** and the driving portion.

The pair of coupling portions **21**B are disposed at positions facing each other across the first axis a_1, and have a shape that is line-symmetrical with respect to the first axis a_1. One end of the coupling portion **21**B is connected to the swing shaft **21**A, and the other end thereof is connected to the movable frame **22**. The coupling portion **21**B has a folded structure. Since the coupling portion **21**B has elasticity due to the folded structure, the internal stress applied to the swing shaft **21**A is relaxed in a case where the mirror portion **20** swings around the first axis a_1.

The second support portion **23** is composed of a swing shaft **23**A and a pair of coupling portions **23**B. The swing shaft **23**A is a so-called torsion bar stretched along the second axis a_2. One end of the swing shaft **23**A is connected to the movable frame **22**, and the other end thereof is connected to the coupling portion **23**B.

On the second axis a_2, there is a gap G**2** between the second support portion **23** and the driving portion.

The pair of coupling portions **23**B are disposed at positions facing each other across the second axis a_2, and have a shape that is line-symmetrical with respect to the second axis a_2. One end of the coupling portion **23**B is connected to the swing shaft **23**A, and the other end thereof is connected to the first actuator **24**. The coupling portion **23**B has a folded structure. Since the coupling portion **23**B has elasticity due to the folded structure, the internal stress applied to the swing shaft **23**A is relaxed in a case where the mirror portion **20** swings around the second axis a_2.

In the mirror portion **20**, a plurality of slits **20**B and **20**C are formed on the outside of the reflecting surface **20**A along the outer periphery of the reflecting surface **20**A. The plurality of slits **20**B and **20**C are disposed at positions that are line-symmetrical with respect to the first axis a_1 and the second axis a_2, respectively. The slit **20**B has an effect of suppressing distortion generated on the reflecting surface **20**A due to the swing of the mirror portion **20**.

In FIGS. **3** and **4**, the wiring line and the electrode pad for giving the driving signal to the first actuator **24** and the second actuator **25** are not shown. A plurality of the electrode pads are provided on the fixed frame **27**.

As shown in FIG. **5**, the MMD **2** is formed, for example, by performing an etching treatment on a silicon on insulator (SOI) substrate **30**. The SOI substrate **30** is a substrate in which a silicon oxide layer **32** is provided on a first silicon active layer **31** made of single crystal silicon, and a second silicon active layer **33** made of single crystal silicon is provided on the silicon oxide layer **32**.

The mirror portion **20**, the first support portion **21**, the movable frame **22**, the second support portion **23**, the first actuator **24**, the second actuator **25**, the first connecting portion **26**A, and the second connecting portion **26**B are formed of the second silicon active layer **33** remaining by removing the first silicon active layer **31** and the silicon oxide layer **32** from the SOI substrate **30** by an etching treatment. The second silicon active layer **33** functions as an elastic portion having elasticity. The fixed frame **27** is formed of three layers of the first silicon active layer **31**, the silicon oxide layer **32**, and the second silicon active layer **33**.

The first actuator **24** includes a piezoelectric element (not shown) formed on the second silicon active layer **33**. The piezoelectric element has a laminated structure in which a lower electrode, a piezoelectric film, and an upper electrode are sequentially laminated on the second silicon active layer **33**. The second actuator **25** has the same configuration as the first actuator **24**.

The upper electrode and the lower electrode are formed of, for example, gold (Au) or platinum (Pt). The piezoelectric film is formed of, for example, lead zirconate titanate (PZT), which is a piezoelectric material. The upper electrode and the lower electrode are electrically connected to the driving controller **4** described above via the wiring line and the electrode pad.

A driving voltage is applied to the upper electrode from the driving controller **4**. The lower electrode is connected to the driving controller **4** via the wiring line and the electrode pad, and a reference potential (for example, a ground potential) is applied thereto.

In a case where a positive or negative voltage is applied to the piezoelectric film in the polarization direction, deformation (for example, expansion and contraction) proportional to the applied voltage occurs. That is, the piezoelectric film exerts a so-called inverse piezoelectric effect. The piezoelectric film exerts an inverse piezoelectric effect by applying a driving voltage from the driving controller **4** to the upper electrode, and displaces the first actuator **24** and the second actuator **25**.

FIG. **6** shows an example in which one piezoelectric film of the pair of second actuators **25** is extended and the other piezoelectric film is contracted, thereby generating rotational torque around the first axis a_1 in the second actuator **25**. In this way, one of the pair of second actuators **25** and the other are displaced in opposite directions to each other, whereby the mirror portion **20** rotates around the first axis a_1.

In addition, FIG. **6** shows an example in which the second actuator **25** is driven in an anti-phase resonance mode (hereinafter, referred to as an anti-phase rotation mode) in which the displacement direction of the pair of second actuators **25** and the rotation direction of the mirror portion **20** are opposite to each other. On the other hand, an in-phase resonance mode in which the displacement direction of the pair of second actuators **25** and the rotation direction of the mirror portion **20** are the same direction is called an in-phase rotation mode. In the present embodiment, the second actuator **25** is driven in the anti-phase rotation mode.

A deflection angle θ of the mirror portion **20** around the first axis a_1 is controlled by the driving signal (hereinafter, referred to as a first driving signal) given to the second actuator **25** by the driving controller **4**. The first driving signal is, for example, a sinusoidal AC voltage. The first driving signal includes a driving voltage waveform V_{1A} (t) applied to one of the pair of second actuators **25** and a driving voltage waveform V_{1B} (t) applied to the other. The driving voltage waveform V_{1A} (t) and the driving voltage waveform V_{1B} (t) are in an anti-phase with each other (that is, the phase difference is 180°).

The deflection angle θ of the mirror portion **20** around the first axis a_1 corresponds to an angle at which the normal line N of the reflecting surface **20**A is inclined with respect to the Z direction in the YZ plane. Hereinafter, the deflection angle θ is also referred to as a rotation angle θ.

The first actuator **24** is driven in an anti-phase resonance mode in the same manner as the second actuator **25**. A deflection angle of the mirror portion **20** around the second axis a_2 is controlled by the driving signal (hereinafter, referred to as a second driving signal) given to the first actuator **24** by the driving controller **4**. The second driving signal is, for example, a sinusoidal AC voltage. The second driving signal includes a driving voltage waveform V_{2A} (t) applied to one of the pair of second actuators **25** and a driving voltage waveform V_{2B} (t) applied to the other. The driving voltage waveform V_{2A} (t) and the driving voltage waveform V_{2B} (t) are in an anti-phase with each other (that is, the phase difference is 180°).

FIGS. **7**A and **7**B show examples of the first driving signal and the second driving signal. FIG. **7**A shows the driving voltage waveforms V_{1A} (t) and V_{1B} (t) included in the first driving signal. FIG. **7**B shows the driving voltage waveforms V_{2A} (t) and V_{2B} (t) included in the second driving signal.

The driving voltage waveforms V_{1A} (t) and V_{1B} (t) are represented as follows, respectively.

$$V_{1A}=V_{off1}+V_1 \sin(2\pi f_{d1}t)$$

$$V_{1B}=V_{off1}+V_1 \sin(2\pi f_{d1}t+\alpha)$$

Here, V_1 is the amplitude voltage. V_{off1} is the bias voltage. f_{d1} is the driving frequency (hereinafter, referred to as the first driving frequency). t is time. α is the phase difference between the driving voltage waveforms V_{1A} (t) and V_{1B} (t). In the present embodiment, for example, α=180°.

By applying the driving voltage waveforms V_{1A} (t) and V_{1B} (t) to the pair of second actuators **25**, the mirror portion **20** swings around the first axis a_1 at the first driving frequency f_{d1}.

The driving voltage waveforms V_{2A} (t) and V_{2B} (t) are represented as follows, respectively.

$$V_{2A}=V_{off2}+V_2 \sin(2\pi f_{d2}t+\varphi)$$

$$V_{2B}=V_{off2}+V_2 \sin(2\pi f_{d2}t+\beta+\varphi)$$

Here, V_2 is the amplitude voltage. V_{off2} is the bias voltage. f_{d2} is the driving frequency (hereinafter, referred to as the second driving frequency). t is time. β is the phase difference between the driving voltage waveforms V_{2A} (t) and V_{2B} (t). In the present embodiment, for example, β=180°. In addition, φ is the phase difference between the driving voltage waveforms V_{1A} (t) and V_{1B} (t) and the driving voltage waveforms V_{2A} (t) and V_{2B} (t). In the present embodiment, for example, $V_{off1}=V_{off2}=0$ V.

By applying the driving voltage waveforms V_{2A} (t) and V_{2B} (t) to the pair of first actuators **24**, the movable portion **60** including the mirror portion **20** swings around the second axis a_2 at the second driving frequency f_{d2}.

The first driving frequency fin is set so as to match the resonance frequency around the first axis a_1 of the mirror portion **20**. The second driving frequency f_{d2} is set so as to match the resonance frequency around the second axis a_2 of the mirror portion **20**. In the present embodiment, the first driving frequency f_{d1} is larger than the second driving frequency f_{d2}.

In a case where the MMD **2** configured as described above is driven two-dimensionally around the first axis a_1 and the second axis a_2, the centrifugal force acting in a case where the movable portion **60** swings around the second axis a_2 serves to assist the swing of the mirror portion **20** around the first axis a_1. The potential energy by the centrifugal force affects the total amount of elastic energy and kinetic energy stored in a case where the mirror portion **20** swings. As a result, a spring constant in the swing of the mirror portion **20** changes and a crosstalk between axes occurs, so that the resonance frequency shifts.

The present applicant found that in a case where the displacement of the second support portion **23** satisfies a predetermined condition in a state where the mirror portion **20** rotates around the first axis a_1 and an absolute value of the rotation angle θ is larger than 0 degrees, the shift of the resonance frequency by the crosstalk between axes is suppressed.

In a case where the displacement of the second support portion **23** satisfies a predetermined condition, a displacement amount of a portion of the movable portion **60** other than the mirror portion **20** increases. As a result, the total amount of elastic energy and kinetic energy in the entire MMD **2** is increased. As a result, the influence of the potential energy by the centrifugal force on the total energy is relatively reduced, and the shift of the resonance frequency by the crosstalk between axes is suppressed.

FIG. **8** is a diagram schematically showing displacement of the second support portion **23** in a case where the mirror portion **20** rotates around the first axis a_1. (A) of FIG. **8** shows a state where the mirror portion **20** is stationary and the rotation angle θ is 0 degrees. (B) of FIG. **8** shows a state where the mirror portion **20** rotates around the first axis a_1 and the absolute value of the rotation angle θ is larger than 0 degrees.

FIG. **8** shows a cross-sectional view of the MMD **2** cut along a plane orthogonal to the first axis a_1 and including the second axis a_2. A straight line α and an intersection C shown in (B) of FIG. **8** are included in the cross section of the MMD **2**. Specifically, the straight line α is a straight line located on the surface of the second support portion **23** and including each end point of the second support portion **23**. The intersection C is a point where the straight line α intersects the second axis a_2.

The total length of the second support portion **23** in the direction of the second axis a_2 in the stationary state is denoted by Lb**1**. In addition, in the direction of the second axis a_2, the distance from an end part of the second support portion **23** on the mirror portion **20** side in the stationary state to the intersection C is denoted by A. Through the experiment described below, the present applicant found that in a case where the distance A is larger than ⅔ times the total length Lb**1** (that is, in a case of ⅔×Lb**1**<A), the shift of the resonance frequency by the crosstalk between axes is suppressed.

In the experiment described below, the present applicant prepared a plurality of samples having different distances A for the MMD **2**, and measured the shift amount of the resonance frequency by the crosstalk between axes by driving each sample. Specifically, a resonance frequency around the first axis a_1 in a case where each sample is driven one-dimensionally around the first axis a_1 (hereinafter, referred to as a first resonance frequency fr**1**) and a resonance frequency around the first axis a_1 in a case where each sample is driven two-dimensionally around the first axis a_1 and the second axis a_2 (hereinafter, referred to as a second resonance frequency fr**2**) were measured. Then, a shift amount Δfr of the resonance frequency by the crosstalk between axes was obtained by calculating a difference between the first resonance frequency fr**1** and the second resonance frequency fr**2**.

FIGS. **9** and **10** show parameters relating to the width, length, and the like of the components of the sample used in the experiment. FIG. **11** is a diagram showing specific setting values of the parameters.

The diameter of the mirror portion **20** was 1.5 mm, the thickness of the SOI substrate **30** was 430 μm, the thickness of the second silicon active layer **33** was 60 μm, and the thickness of the silicon oxide layer **32** was 40 μm. The length of one side of the fixed frame **27** was 5.2 mm.

The present applicant used Xac**2** and Yac**2** as variables among the parameters shown in FIG. **11**. That is, the present applicant prepared a plurality of samples having different distances A by changing the lengths of Xac**2** and Yac**2** for each sample.

Modification Example

As Modification Example, the present applicant prepared samples for an MMD **2**A in which the shape and the like of the components are different from those of the MMD **2** according to the above embodiment.

FIG. **12** shows the configuration of the MMD **2**A according to Modification Example. In FIG. **12**, the components having the same functions as those of the MMD **2** according to the above embodiment are designated by the same reference numerals. In the MMD **2**A, a connecting portion **26** is provided instead of the first connecting portion **26**A and the second connecting portion **26**B. The connecting portion **26** is provided on the first axis at, and connects the first actuator **24** to the second actuator **25** and connects the second actuator **25** to the fixed frame **27**.

FIGS. **13** to **15** show parameters relating to the width, length, and the like of the components of the MMD **2**A. FIG. **16** is a diagram showing specific setting values of the parameters.

In Modification Example, the diameter of the mirror portion **20** was 1.5 mm, the thickness of the SOI substrate **30** was 350 μm, the thickness of the second silicon active layer **33** is 60 μm, and the thickness of the silicon oxide layer **32** was 65 μm. The length of one side of the fixed frame **27** was 5.2 mm.

Experimental Result

For the above-described embodiment and modification example, each sample was driven in a vacuum chamber to measure the first resonance frequency fr**1** and the second resonance frequency fr**2**. Specifically, the driving frequency was swept while irradiating the mirror portion **20** during driving with laser light, and the driving frequency at which a spreading angle of reflected light was maximized was measured as the resonance frequency. In addition, the deflection angle of the mirror portion **20** was calculated from the spreading angle of the reflected light.

FIG. **17** shows measurement results of the first resonance frequency fr**1** and the second resonance frequency fr**2** for each sample. Sample number **1** indicates a sample prepared for the MMD **2**A according to Modification Example. Sample numbers **2** to **9** indicate samples prepared for the MMD **2** according to the embodiment. Sample numbers **2** to **9** have different lengths of Xac**2** and Yac**2**.

The first resonance frequency fr**1** is a resonance frequency during one-dimensional driving in a case where the deflection angle of the mirror portion **20** around the first axis a_1 is ±1.25 degrees. The second resonance frequency fr**2** is a resonance frequency during two-dimensional driving in a case where the deflection angle of the mirror portion **20** around the first axis a_1 is ±1.25 degrees and the deflection angle of the mirror portion **20** around the second axis a_2 is ±11.5 degrees. The shift amount Δfr of the resonance frequency is a value obtained by subtracting the first resonance frequency fr**1** from the second resonance frequency fr**2**.

The distance A was measured for each sample using a laser Doppler vibrometer. Then, using the measured distance A, a ratio A/Lb**1** of the distance A to the total length Lb**1** of the second support portion **23** was calculated.

In a case where an application to a laser display for AR glasses is considered, an appropriate value of the deflection angle of the mirror portion **20** around each axis during the two-dimensional driving is ±17 degrees around the first axis a_1 and ±11.5 degrees around the second axis a_2. Therefore, for each sample, it was determined whether or not the two-dimensional driving was possible stably for 60 seconds or longer while maintaining the deflection angle at an appropriate value. The term "OK" indicates that the stable two-dimensional driving for 60 seconds or longer was possible. The term "NG" indicates that the stable two-dimensional driving for 60 seconds or longer was not possible.

The power consumption of each sample was measured using a current probe in a state where the sample was resonated by the one-dimensional driving around the first axis a_1. In this case, the deflection angle of the mirror portion **20** around the first axis a_1 was ±17 degrees.

According to the experimental results shown in FIG. **17**, it can be seen that the larger the ratio A/Lb**1**, the smaller the shift amount Δfr of the resonance frequency. The small shift amount Δfr means that an absolute value of the shift amount Δfr is small. In addition, it can be seen that in a case where the ratio A/Lb**1** is larger than ⅔ (greater than about 0.66), the two-dimensional driving is stabilized, and the superiority can be obtained from the viewpoint of the application to the laser display for AR glasses. FIG. **18** is a graph showing dependence of the shift amount Δfr of the resonance frequency on the ratio A/Lb**1**.

FIG. **19** is a graph showing dependence of power consumption on the ratio A/Lb**1**. Low power consumption is desirable for a general laser display application. As a guide, in a case where the power consumption during the one-dimensional driving is 80 mW or less, a certain degree of superiority as a laser display application can be secured. Therefore, it can be seen that in a case where the ratio A/Lb**1** is 6/5 or less (1.2 or less), the power consumption is 80 mW or less, and a certain degree of superiority can be secured from the viewpoint of the power consumption.

That is, it is preferable that the ratio A/Lb**1** satisfies a relationship of ⅔<A/Lb**1**. Further, it is preferable that the ratio A/Lb**1** satisfies a relationship of ⅔<A/Lb**1**<6/5.

FIG. **20** shows the simulation results. (A) to (C) of FIG. **20** show that the lengths of Xac**2** and Yac**2** are different. The intersection C corresponds to a point where the displacement of the second support portion **23** is zero. It can be seen that the position of the intersection C changes (that is, the distance A changes) according to the lengths of Xac**2** and Yac**2**. Also in the simulation, it was confirmed that the larger the ratio A/Lb**1**, the smaller the shift amount Δfr of the resonance frequency.

In the above embodiment, the hardware configuration of the driving controller **4** can be variously modified. The processing unit of the driving controller **4** may be composed of one processor or may be composed of a combination of two or more processors of the same type or different types. The processor includes, for example, a CPU, a programmable logic device (PLD), or a dedicated electric circuit. As is well known, the CPU is a general-purpose processor that executes software (program) to function as various processing units. The PLD is a processor such as a field programmable gate array (FPGA) whose circuit configuration can be changed after manufacture. The dedicated electric circuit is a processor that has a dedicated circuit configuration designed to perform a specific process, such as an application specific integrated circuit (ASIC).

All documents, patent applications, and technical standards mentioned in this specification are incorporated herein by reference to the same extent as in a case where each document, each patent application, and each technical standard are specifically and individually described by being incorporated by reference.

What is claimed is:

1. A micromirror device comprising:

a mirror portion on which a reflecting surface for reflecting incident light is formed;

a pair of first support portions, each of which is connected to the mirror portion on a first axis located in a plane including the reflecting surface of the mirror portion in a stationary state, and swingably supports the mirror portion around the first axis;

a pair of movable frames that are respectively connected to the pair of first support portions and face each other across the first axis;

a pair of second support portions, each of which is connected to a corresponding one of the pair of movable frames on a second axis which is located in the plane including the reflecting surface of the mirror portion in the stationary state and is orthogonal to the first axis, and each of which includes a swing shaft that swingably supports a movable portion including the mirror portion, the first support portions, and the pair of movable frames around the second axis;

a driving portion that surrounds the movable portion and has a gap with each of the pair of second support portions on the second axis;

a pair of coupling portions included in each of the pair of second support portions, and configured to couple the swing shaft and the driving portion; and

a fixed frame that is connected to the driving portion and surrounds the driving portion,

wherein, in a state where the mirror portion rotates around the first axis and an absolute value of a rotation angle is larger than 0 degrees,

assuming that, in a plane orthogonal to the first axis and including the second axis, a distance between an intersection between the second axis and a straight line located on a surface of the swing shaft and including each end point of the swing shaft and an end part of the swing shaft on a mirror portion side in the stationary state is denoted by A, and a total length of the swing shaft in a direction of the second axis is denoted by L, a relationship of $2/3<A/L$ is satisfied.

2. The micromirror device according to claim **1**,

wherein the driving portion has a piezoelectric element.

3. The micromirror device according to claim **1**,

wherein the driving portion includes

a pair of first actuators facing each other across the second axis and having a piezoelectric element, and

a pair of second actuators surrounding the first actuator, facing each other across the first axis, and having a piezoelectric element.

4. The micromirror device according to claim **3**,

wherein the pair of second actuators allow the mirror portion to swing around the first axis, and

the pair of first actuators allow the movable portion to swing around the second axis.

5. The micromirror device according to claim **1**,

wherein the distance A and the total length L satisfy a relationship of $2/3<A/L<6/5$.

6. An optical scanning device comprising:

the micromirror device according to claim **1**; and

a processor that drives the driving portion,

wherein the processor allows the mirror portion to swing around the first axis and the second axis by providing a driving signal to the driving portion.

* * * * *